Direct fuel cell—supercapacitor hybrid power source for personal suburban transport

Caroline Bonnet[1], Stéphane Raël[1,2,*], Melika Hinaje[2], Sophie Guichard[2], Théophile Habermacher[3], Julian Vernier[3], Xavier François[4], Marie-Cécile Péra[5], François Lapicque[1]

[1] Université de Lorraine, CNRS, LRGP, F-54000 Nancy, France
[2] Université de Lorraine, GREEN, F-54000 Nancy, France
[3] H2Sys, Campus of the Technology University of Belfort Montbéliard, rue Thierry Mieg, F-90000 Belfort, France
[4] FCLAB, Univ. Bourgogne Franche-Comté, CNRS, UTBM, Belfort, France
[5] FEMTO-ST Institute, FCLAB, Univ. Bourgogne Franche-Comté, CNRS, Belfort, France

*** Correspondence:** Email: stephane.rael@univ-lorraine.fr.

Abstract: In view to proposing an alternative to oversized energy sources currently installed in electric vehicles for suburban transport, a direct hybrid fuel cell (FC)-supercapacitors (SC) source has been designed and tested on a test bench. The rated 15.6 kW source—with an air-cooled 5.6 kW FC and a 165 F SC storage device—was shown perfectly suited to traction of a 520 kg vehicle along the NEDC cycle, then validating the previously developed concept of a one-ton car propelled by a 10 kW FC in the rated 30 kW hybrid source for this cycle. In comparison with a FC used alone, hybridization was shown to allow the power demand for the cell to vary in quite a narrower range, as formerly observed. Moreover, the rates of fuel cell voltage and current generated in the driving cycle, were shown to be reduced by one order of magnitude by the direct hybridization which is to contribute to the FC durability. Two operating parameters were shown to have a significant effect on the hybrid source efficiency, namely the capacity of the SC at 110 or 165 F, and the recovery of deceleration power—emulated by an external power supply—which can decrease by 25% the fuel consumption in NEDC cycle conditions, as predicted by the model.

Keywords: direct hybridization; driving cycles; fuel cell systems; supercapacitors; transportation.

1. Introduction

Polymer electrolyte membrane fuel cells (PEMFCs) have been considered for years for transported applications. However, a fuel cell alone although powerful, cannot easily bring the considerable initial electric power required to start up the vehicle [1,2]. Moreover, the FC stack installed in the vehicle cannot store the regenerative power produced during decelerating and braking. Third, operation under idle conditions or sudden changes in the fuel cell current or power and currents in usual driving cycles, are to cause appreciable degradation of the FC components [3–7]. Fuel cell hybridization by energy storage elements e.g., batteries or supercapacitors can mitigate the three above intrinsic weaknesses of fuel cells in transport applications. As a matter of fact, the buffering action of

energy storage elements in the hybrid source, is to avoid fuel cell operation under idle conditions or sudden changes in its power demand which is to favor the fuel cell durability. Their capacity in energy storage differs greatly with their nature. Typically, supercapacitors (SCs) offer higher dynamics in the storage and power release than batteries but lower available energy, even though recent battery technologies with supercapacitor anodes can tolerate higher charge/discharge rates. Batteries will be preferred for long-distance or versatile rides, whereas SC can be attractive for rides with frequent changes in the power demand, as in (sub)urban transport. An additional interest of hybridization is the enhancement of the power allowed, in particular when the braking energy of the vehicle is partly recovered to contribute to recharging the storage elements.

Hybridization can be carried out in an active (indirect) manner using DC-DC converters to decouple the FC or the energy storage system, or both, and after development of energy management strategies (EMS). This solution more complex and involving additional components in the powertrain circuit and subsequent energy losses, is known to better protect the hybrid source (HS) components from operation under hazardous conditions [8]. With direct (passive) hybridization i.e., without any interface converter, energy exchanges within the hybrid source are ruled by the mere association of the fuel cell to the storage element, thus by the voltage vs. current relationship of the two source components connected in parallel ([9], Jacome (2021). The storage elements have to be pre-charged beforehand to avoid initial hazardous inrush currents at the closure of the electrical circuit. Moreover, a diode inserted in the circuit after the fuel cell provides it a minimal protection. Although less flexible in the energy management of the hybrid source, passive hybridization appears attractive because of its simplicity, its lower weight and its expected higher energy efficiency, as discussed in [6,9,10].

Depending on the vehicle considered and its targeted use, hybrid sources have been tested with dedicated driving cycles to utility vehicles [11], urban cycles [12], or more versatile cycles covering urban or sub-urban driving e.g., NEDC [13,14], or even short highway driving HWFET [15]. Most investigations cover the design of the several kW-rated hybrid source, relying upon force and power balances to mitigate the various friction forces exerted on the vehicle, together with the dynamics to be offered by the hybrid source for the targeted application. Both the hybrid source components and the powertrain system are often modeled with equivalent circuit models, the transients of the current and powers profiles being in some cases validated by experiments. Besides, in direct hybridization the SC storage device has to be pre-charged for the above safety reasons, and various strategies have been proposed for this purpose [6,10,16,17]. Durability of the fuel cell has also been investigated, either by estimation of the degradation of the fuel cell components [9] using semi-empirical laws established in dedicated experimental tests [18,19], or in long-term runs of a single hybridized fuel cell in FC-DLC driving cycles. There, the regular assessment of the fuel cell state of health revealed that direct hybridization to a SC module can slightly protect the fuel cell or at least does not accelerate its degradation [20–22]. Aside durability aspects, it has been shown that the fuel cell could be significantly downsized upon its hybridization, depending on the capacitance of the storage system [8–12,23]): appreciable reduction in the costs for the FC investment and maintenance can thus be expected. However, the contribution of regenerative power of the vehicle deceleration in the energy management, although sometimes mentioned, was seldom investigated [12].

The present work has been carried out in view to operating an individual electric vehicle (1000 kg), with a direct hybrid (FC-SC) source for urban/sub-urban driving (Hy2Car project, Nancy, France), and relying upon previously gained experience at bench scale [20,21]. The objective of the whole Hy2Car project, is to propose an alternative personal vehicle with a modest hydrogen demand, low

emission and undersized powertrain suitable to urban/suburban driving. In this work dedicated to half-scale investigation of the above vehicle, a max. 16 kW direct FC-SC hybrid source comprising a 6-kW fuel cell, has been designed using previous small-scale studies [24] and relying upon previously developed physics-based models of fuel cells [25] and supercapacitors [26]. More details on these models can be found in the appendix. On the basis of the design of its storage system in terms of rated voltage and capacitance, the above hybrid source was tested with NEDC driving cycles at the FClab platform in Belfort. Contrary to former works quoted, the power of the hybrid source and the weight of the fictitious vehicle have been varied for more complete investigation of the behavior of the hybrid source-vehicle system. Two dynamics of the source have therefore been considered in the present study by varying the number of SC modules directly connected to two 3 kW Ballard fuel cells in series. The vehicle with a fictitious weight varying from 400 to 520 kg, has been simulated using suitable data and laws for mechanical friction of electric vehicles. Energy sharing between the fuel cell and the SC has been followed, in repeated driving cycles. Interestingly, the energy recovered in deceleration periods was shown to represent up to 25% of the hybrid source power. Besides, the rates of the fuel cell voltage and current in NEDC cycles was estimated, providing indication on the stress induced on the fuel cell depending on the hybridization mode.

2. Experimental section and methodology development

2.1. Materials and experimental tests

2.1.1. The fuel cell system

A fuel cell system has been developed by H2Sys company, Belfort, on the basis of two fuel cell stacks (Ballard version EOM 3000 W with air cooling) connected in series. Each stack consisted of 80 cells with an area at 145 cm^2. Air was supplied by forced convection with ambient atmosphere and hydrogen was supplied upon pressure (8 bars) upstream to the fuel cell operated in dead-end mode, with automatic release of the anode gases (purge) upon action of the controlling system developed. The fuel cell system was equipped with a CAN bus J1939 2.0 interface to check the various physical variables on a laptop. In particular, the fan power for air cooling was adjusted depending on the temperature of each stack to avoid overheating of the cell. Current was kept below 65 A to avoid temperatures over 62 °C as recommended by the FC supplier. The fuel cell system comprising 160 single cells, could deliver an electric power up to 5.6 kW with a voltage ranging from 89 V to 146 V. Figure 1 depicts the overall experimental setup covering the two fuel cells, the supercapacitor strings and the other electrical components.

2.1.2. *Supercapacitor storage devices*

SC storage devices have been prepared by assembling in parallel and in series 165 F–48.6 V supercapacitor modules from Maxwell Technologies company. Each module, of BMOD0165P048 type, was composed of 18 cells in series whose cell capacitance, rated voltage and mass were 3000 F, 2.7 V and 500 g, respectively. The weight of one module was near 14 kg, and its series resistance was measured at 6 mΩ. The first SC storage device used for direct hybridization with the above fuel cell system was formed with two paralleled strings of three modules in series, for a nominal capacitance

of 110 F and a rated voltage at 145.8 V. The second one with three paralleled strings of three modules in series, offered a capacitance of 165 F for the same rated voltage. The total weight of the packed storage devices attained 84 kg and 126 kg, respectively, corresponding to a net SC cell weight near 54 kg and 81 kg, respectively.

Prior to connecting the SC storage device to the fuel cell, pre-charging of the supercapacitors was carried out using a power supply EA 200 V/210 A to adjust the initial voltage to a level compatible to that of the fuel cell.

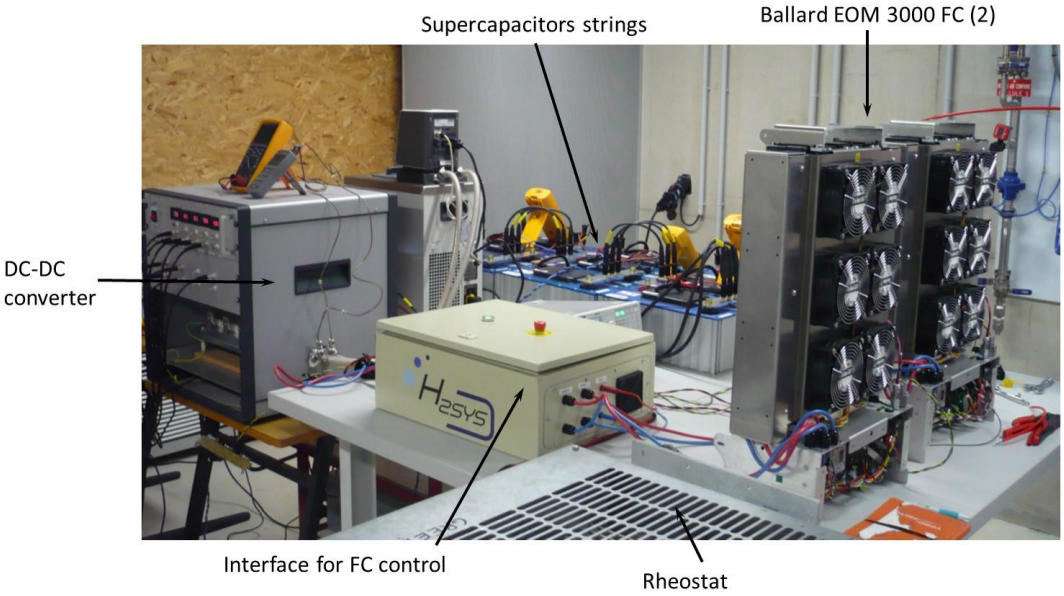

Figure 1. Experimental setup.

2.1.3. *The electrical setup and its operation*

The electrical scheme of the experimental setup is more precisely depicted in Figure 2. The fuel cell was protected from negative currents by a diode. The hybrid source was loaded by a power electronic DC-DC converter composed of two phases in order to achieve power conversion up to 40 kW. Each phase has an inductive input (inductance: 400 µH rated at 125 A), and involves an IGBT half-bridge module of SKM400GB066D type (rated at 600 V–400 A) from Semikron company. Both phases were current reversible, allowing to emulate the recovery mode. The phase currents were controlled by means of regulation loops, so that the hybrid source current I_{HS} could be set to a given value or profile. The hybrid source components were connected to each other by 125 A Staubli cables. The wiring between the supercapacitive storage device and the power converter was doubled to reduce the significance of ohmic voltage drop and undesired Joule effects, as hybrid source current I_{HS} was expected to be as large as 250 A. The electric energy produced by the hybrid source was dissipated in two paralleled rheostats (each being rated at 4 Ω, 60 A and 14.4 kW), through a braking chopper connected to the converter DC link. Finally, the recovery (regeneration) of the deceleration-braking energy was emulated in cycling tests by means of the above power supply.

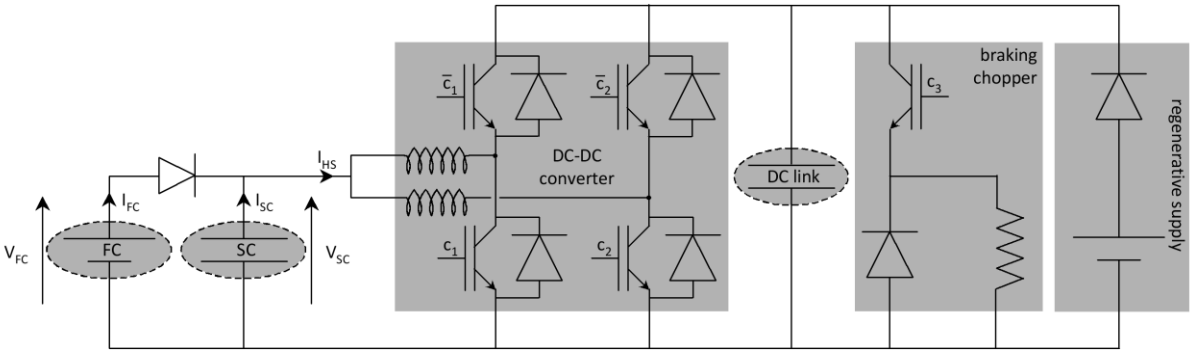

Figure 2. Electrical scheme of the experimental setup.

The DC-DC converter phases were driven by means of current regulation loops, in order to control the hybrid source current I_{HS}. The reference signal I_{HSREF} for this current was computed from the NEDC speed profile, according to the mechanical power demand detailed in section 2.2. The braking chopper, whose general purpose is to manage the consumption of the energy produced by the hybrid source (corresponding current regime: HIS > 0), was simply driven by a hysteresis comparator, as to maintain the DC link voltage below a given level (160 V here), which must be higher than the maximum voltage attainable by the hybrid source. When required for recovery braking emulation (corresponding current regime: HIS < 0), the power supply was connected to the DC link through a diode, and its output voltage was set to 155 V, i.e., between the highest HS voltage and the limit for the DC link voltage at 160 V.

The test bench supervision (DC-DC converter control, braking chopper control, computation of power and current references of the hybrid source, safety shutdown), was managed by two dSPACE® real time cards (computation sample time: 100 µs), in combination with Controldesk® software and Matlab-Simulink® environment. These cards also allowed data acquisition and backup of FC, SC and HS currents and powers, together with FC, SC and DC link voltages, with a 100 ms acquisition sample time. Switching noises generated by the power electronic conversion (switching frequency: 10 kHz) were removed by first-order low-pass filters with a cut-off frequency of 100 Hz in the measurement of the hybrid source currents (I_{FC}, I_{SC} and I_{HS}) and voltages (V_{FC} and V_{SC}).

2.2. Model for vehicle traction and estimation of the power demand

The NEDC cycle in the form of a velocity time profile consists of four short urban cycles with a maximum velocity of 50 km/h, and four peaks in suburban acceleration phases with velocity up to 70, 70, 100 and 120 km/h—for a few seconds for the last peak. The 1180 s long cycle covers 10.93 km with an average velocity near 33 km/h. A model has been developed to calculate the instantaneous power demand of the fictitious vehicle from the velocity profile of the cycle. This power demand corresponds to the mechanical power of the vehicle at velocity v, considering efficiency η for conversion of electrical power to mechanical power.

The mechanical model was established by expressing the instantaneous mechanical power P_{mech} of the vehicle in motion, as the sum of the variation of the mechanical energy (kinetic and potential) of the vehicle, and the dissipation terms related to friction forces, as follows:

$$P_{mech} = M.v.\frac{dv}{dt} + M.g.v.\sin(\alpha) + F_F.v \quad (1)$$

where M the mass of the vehicle, g the gravity, α the angle of the slope counted positive (uphill) or negative (downhill), and F_F covers all friction forces. Here, angle α was taken at 0°, assuming in this study driving in flat areas, because no changes in elevation are accounted for in NEDC cycles. Friction forces are usually considered as due to internal friction in the car and on the road, F_w, and to friction to air, F_a:

$$F_F = F_w + F_a = f_w.M.v + \frac{1}{2}\rho_a.S.C_x.v^2 \quad (2)$$

where f_w is the vehicle friction coefficient, ρ_a the density of air, S the cross sectional area of the vehicle in motion and C_x its drag coefficient. The vehicle was assumed to have the same friction characteristics as the Renault Zoe, an electrical vehicle for which available data can be found on the web. For Renault Zoe:

$$M = 1480 \text{ kg}, f_w = 0.0072 \text{ s}^{-1}, \text{ and product } (S.C_x) \text{ is equal to } 0.75 \text{ m}^2 \quad (3)$$

Conversion of electrical power into mechanical power induces additional losses which were evaluated from the parameters of the Zoe vehicle as follows. The 41 kWh of energy contained in the batteries of the considered version of Zoe vehicle allows a driving NEDC range near 400 km, i.e., 36.6 cycles. The average power in the cycle can then be deduced from the number of cycles and the 1180 s period per cycle: P_{cycle}=3419 W. From the Saber® model developed [24], the average power required in a cycle was estimated at 3148 W, with a mechanical mean contribution from the car engine at P_{mech} = 4324 W, and an average value for the regenerated power from deceleration at $P_{recovery}$ = −1176 W [24]. Assuming the same energy efficiency η for the conversion of mechanical to electrical energies and the reverse operation, P_{cycle} can be written as:

$$P_{cycle} = \frac{P_{mech}}{\eta} + \eta.P_{recovery} \quad (4)$$

The energy conversion efficiency was then found at 95.3%. The electric power recovered in deceleration was found at 1120 W, thus offering to 25% reduction in the power required.

Because the hybrid source has a power far below that required by a Zoe vehicle for the driving cycle of interest, a vehicle of weight M (kg), M being an operating parameter, was considered in this work. Energy and powers have been therefore expressed per mass unit (kg). The air friction force has been assumed to be proportional to the mass of the vehicle, on the basis of the above data for the 1480 kg of the Zoe vehicle.

The power to be supplied by the hybrid source could then be calculated from the above mechanical model. Figure 3 presents the resulting mass power profile (in $W.kg^{-1}$), together with the velocity profile in the NEDC driving cycle: Table 1 summarizes the main power features of this profile. For tests without power recovery in deceleration, the lowest power of the hybrid source is 0, whereas it is obviously negative with recovery of deceleration power. In all cases, the reference signal I_{HSREF}

required for the control of the hybrid source current, was computed by dividing the power profile by the hybrid source voltage, V_{FC}.

For fictitious weight M and given conditions of hybridization (capacitance of the storage device) and energy management (with or without energy recovery in deceleration), the hybrid source was operated following two constraints as follows. First, sufficient power is required to meet the various peaks of power demand, in particular the final one emulating a peak velocity at 120 km/h. Secondly, the power from the fuel cell was restricted by the maximum current fixed at 65 A to avoid its accelerated degradation. For the hybrid source used here, weight M was thus found to be lower or equal to 415 kg with the smaller SC storage device (capacitance: 110 F) and to 520 kg with the larger one at 165 F (see appendix).

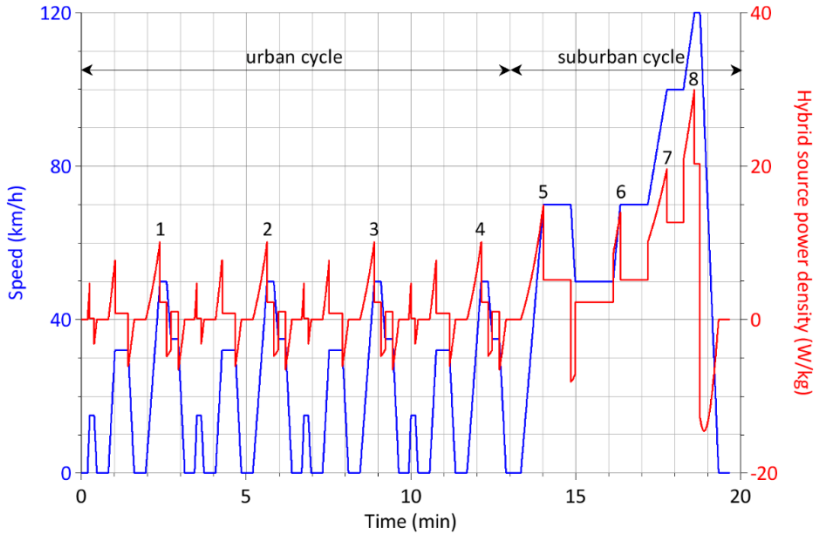

Figure 3. Velocity and mass power profiles along a NEDC driving cycle. Peaks 1 to 8 correspond to the power demand peaks, from 1 to 4 in the urban driving phases below 50 km/h, peaks 5 to 8 being for the suburban part of the cycle, with higher velocities.

Table 1. Power features of the NEDC cycles for a Zoe-like vehicle.

	P_{HS} max. (W/kg)	P_{HS} min. (W/kg)	P_{HS} aver. (W/kg)
without recovery of the deceleration power	30.02	0	3.08
with recovery of the deceleration power	30.02	−14.52	2.32

2.3. Polarization curve of the fuel cell system

This relationship has been experimentally determined by measuring the steady voltage of the fuel cell system alone at a given current. Current was increased from 0 A (open-circuit voltage) to 65 A with 5 A step, then reduced back to 0 A, under comparable current step variations. Steady voltage of the FC was usually obtained after one minute or so. Because of the cooling system of the fuel cell, the temperature depended strongly on the cell current, passing from 25 °C at open circuit voltage to nearly 60 °C for the maximal current. However, as shown in Figure 4, a hysteresis in the voltage variations was observed, with slightly larger voltages reported in the reverse (downward) current scan. The voltage difference in hysteresis up to 20 mV/cell at 40 A, was presumably due to higher hydration of

the ionomer of the membrane and at the catalyst surface, and to highly changing temperature levels. The polarization data in this figure are representative of the fuel cell behavior checked every day during the experiment campaign. The average variation of the downward and upward variations was taken into account for fitting. The following law had been considered (per cell), with a temperature fixed arbitrarily at 40 °C, for which the equilibrium cell voltage U_0 was taken at 1.21 V.

$$U_{FC} = \frac{V_{FC}}{N} = U_0 - r_{cell} i - \frac{RT}{\alpha_a F} asinh\left(\frac{i}{2i_{0,a}}\right) - \frac{RT}{\alpha_c F} asinh\left(\frac{i}{2i_{0,c}}\right) + \frac{RT}{F} Ln\left(1 - \frac{i}{i_L}\right) \quad (5)$$

The values for the various kinetic parameters are reported in Table 2. The fitted U_{FC} vs. I variations are shown in Figure 4.

Table 2. Parameter averaged values for the polarization curve of the fuel cell system Ballard EOM 3000 W.

r_{cell} ($\Omega.cm^2$)	α_a (-)	α_c (-)	$i_{0,a}$ ($A.cm^{-2}$)	$i_{0,c}$ ($A.cm^{-2}$)	i_L ($A.cm^{-2}$)
0.125	2	0.5	0.5	$2.8\ 10^{-5}$	0.5

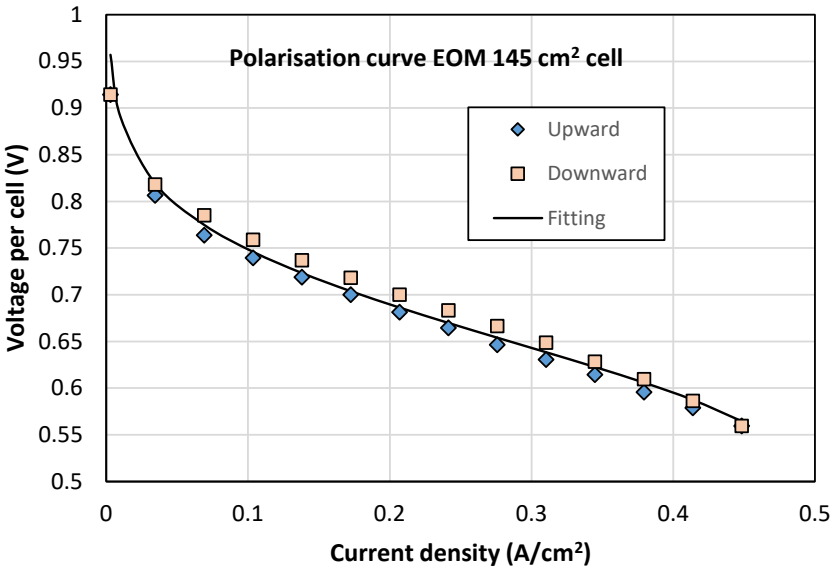

Figure 4. Typical polarization curves of one single cell of the FC system.

3. Results and discussion

Various experimental tests had been carried out with two levels of hybridization capacitance (110 and 165 F), different power profile magnitudes (i.e., different values for the vehicle weight M), and with or without energy regeneration during deceleration phases. For each test condition considered, three cycles were performed. The first cycle corresponded to the transient operation of the hybrid source, for which the energy contributions of the fuel cell and of the SC were affected by the initial state of the hybrid source. On the contrary, the second and the third cycles were usually found very similar to each other, with a stack voltage difference at a given time below 200 mV, i.e., less than 0.2%

of its average value. Treatment and interpretation of the data were achieved on the third cycle, considered to represent steady operation of the hybrid source in NEDC driving cycles.

3.1. General effects of the direct hybridization

3.1.1. General trends

Due to direct hybridization, the voltages of the fuel cell system and the SC storage device are to be by principle identical: here they only differed from each other by less than 1 V, because of the ohmic drop in the wires and the presence of the semi-conductor diode protecting the fuel cell. Figure 5 reports an example of currents and powers of the fuel cell, the SC storage device and the hybrid source. For this case without recovery of the deceleration power, current and power of the hybrid source were positive. They exhibit sharp peaks in urban circuits in the first 800 s of the cycle, and still sharper variations in the second part of the cycle, for the suburban driving section. As observed in former quoted works, for low power demands, the fuel cell operates at a substantial regime, allowing the SC to be recharged, whereas high power demands in the NEDC cycle benefit from the effective contribution of the SC, in particular in the highest peak corresponding to the 120 km/h driving section. The filtering effect of hybridization on the fuel cell power was also observed here. The contribution of supercapacitors in the power demand, was as expected positive or negative depending on the power demand, with an average current over one cycle usually below 0.2 A (absolute value), corresponding to an average (absolute) power below 30 W. This value represents approximately 0.2% of the hybrid source power, in the range 12–16 kW, depending on the size of the SC storage device: this confirms the fact that the hybrid source attained in the third cycle a well-established cycling regime.

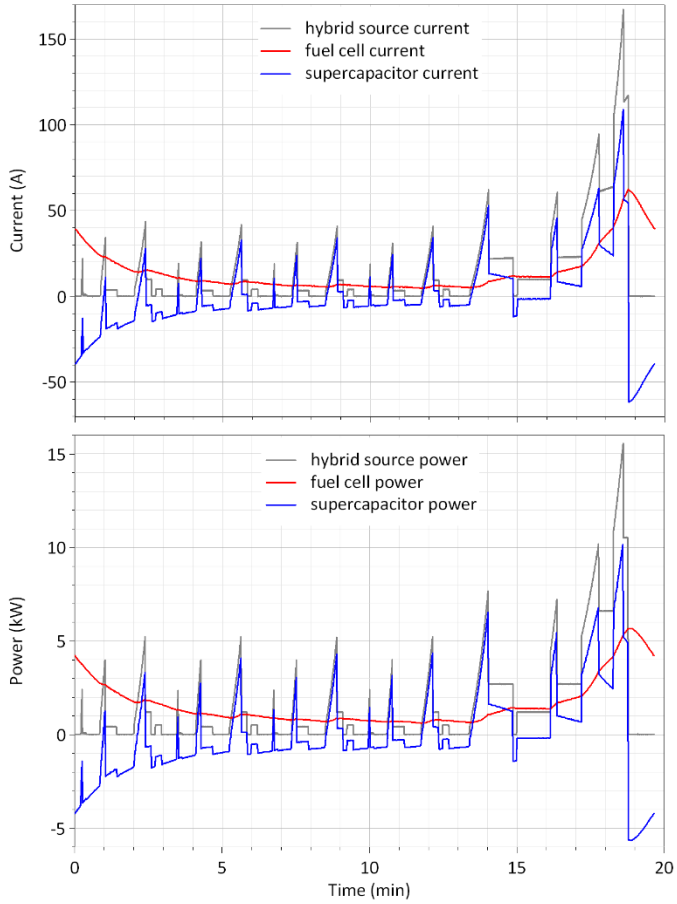

Figure 5. Fuel cell, supercapacitor and hybrid source currents and powers along a NEDC cycle. Conditions: M = 520 kg, SC capacitance: 165 F, no recovery in deceleration.

3.1.2. Quantified effects on currents and powers

Depending on test conditions, the minimum value of the fuel cell current varied from 1.4 A to 4.4 A, i.e., from 0.01 A.cm^{-2} to 0.03 A.cm^{-2}. Corresponding maximum voltage of the FC system remained in the range 129.6–134.9 V, i.e., from 0.810 to 0.843 V per cell. In comparison, the non-hybridized FC had an open circuit voltage near 146 V (0.914 V/cell). Although to a moderate extent, hybridization is to reduce the oxidizing stress on the fuel cell components in the idle periods of the cycle.

The average fuel cell current was in the range 7.9 A–14.3 A, corresponding to an average power of this component varying from 0.95 kW to 1.63 kW (respectively observed for 400 kg/165 F/with recovery, and 520 kg/165 F/without recovery). As demonstrated in previous works [21,23], the ratio $I_{FC,RMS}/I_{FC,MEAN}$ between the RMS and the average fuel cell currents, in addition to being related to fuel cell efficiency, can be used as an indicator of the filtering effect introduced by the storage device. This ratio was approximately equal to 1.5 with a storage device at 110 F, and to only 1.3 at 165 F. In comparison, the non-hybridized FC would have exhibited the theoretical ratio at 2.

To quantify the benefit of direct hybridization, in terms of either power downsizing of the fuel cell system, or power contribution splitting at load peaks, one can introduce the power ratio of the hybrid source over the contribution from the fuel cell, called hybridization ratio. This ratio mainly depends on the power profile, on the capacitance of the storage device, and to much a lower extent on

recovery conditions. It can be first defined as "global", as $P_{HS,MAX}/P_{FC,MAX}$ over the whole NEDC cycle. In this case, the hybridization ratio is representative of the FC power downsizing level. However as seen in Figure 5, maxima of FC and HS power profiles do not occur at exactly the same time in the cycle: the highest power from the hybrid source is supplied in the last seconds of the acceleration period to reach the peak velocity at 120 km/h, whereas the peak power from the fuel cell is given at the end of the 120 km/h plateau, i.e., 10 seconds later. The global hybridization ratio attained 2.15 with the 110 F storage device, and 2.78 with the 165 F storage device. In other words, in spite of the limited energy stored in supercapacitors (energy density below 5 Wh/kg) compared to lithium-ion batteries, and the absence of interface converter for efficient management of power and energy in the hybrid source, hybridizing directly a FC system with a SC storage device offers significant FC downsizing capabilities.

Since Sept. 2017, the NEDC qualification procedure for light vehicles has been gradually replaced by the worldwide harmonized light vehicles test procedures (WLTP), comprising three test cycles, depending on vehicle peak power density P_m: WLTC-1 for $P_m \leq 22$ W.kg^{-1}, WLTC-2 for $22 < P_m \leq 34$ W.kg^{-1}, and WLTC-3 for $P_m > 34$ W.kg^{-1}. The hybrid source considered here corresponds to the second cycling profile requirements. Although no experiments have been up to now carried out with WLTP profiles, the behavior of the hybrid source in WLTP speed profiles has been simulated using the experience with NEDC cycle. Details in the hybrid source modeling are reported in [23], and summarized in the appendix. Under WLTC-2 profile (duration: 1477 s, maximum velocity: 85.2 km/h), with 165 F and no power recovery, the global hybridization ratio was found at 2.92. Moreover, because of the significantly lower max. velocity compared to that in NEDC, weight M could be taken at 1 ton with the above hybrid source (see appendix), i.e., two times more than that considered at the bench for NEDC cycles (Figure 5).

Hybridization benefits can also be discussed in terms of "local" hybridization ratios, i.e., calculated at each load peak, which enables to examine the evolution of power contribution splitting along the cycle. Table 3 summarizes the ratio values obtained for the eight major load peaks shown in Figure 3, with peaks (1–4) in the urban phase and peaks (5–8) in suburban acceleration phases. Local ratios attained values ranging from 4 to 7 in phases of moderate power demand (peaks 2 to 6), and still near 3 in periods of high power demand (peaks 7 and 8). The lowest value, close to 2.8, is obtained at the beginning of the cycle (peak 1), after the high power demand of the previous cycle: the fuel cell is then submitted to quite high power production, for the intense recharging of the SC system.

Table 3. "Local" hybridization ratios calculated at NEDC load peaks. Conditions: M = 520 kg, SC capacitance: 165 F, no recovery in deceleration.

	urban load peaks				*suburban load peaks*			
	1	*2*	*3*	*4*	*5*	*6*	*7*	*8*
P_{FC} [kW]	1.88	1.09	0.87	0.78	1.07	1.69	3.36	5.30
P_{HS} [kW]	5.24	5.24	5.23	5.24	7.70	7.24	10.2	15.6
P_{HS}/P_{FC} [-]	2.79	4.81	6.01	6.72	7.20	4.28	3.04	2.94

Another aspect of the direct hybridization is the state of charge (SOC) of the supercapacitors along the driving cycle. For these energy storage systems, SOC is a linear function of their voltage. As shown in Figure 6 for the highest power profiles (M = 520 kg, SC capacitance: 165 F, with and without

recovery in deceleration), SOC usually varied from 61% to 89% or 91%, respectively without or with recovery. Corresponding average SOC were near 84% and 86%.

The min. SOC value may appear high for usual energy storage systems, but the value directly derives from the highest FC current at 65A, corresponding to the min. voltage at 89V. Because SC and FC voltages are very close to each other in direct hybridization, this leads to the min. SOC value at 89/145.8 (100% SOC being set at the storage device rated voltage), i.e., 61%. This does not represent an additional constraint in operating direct SC-FC hybridization, but this only limits the SOC range of the storage device. Minimum SOC in the order of 50% are usually considered with supercapacitors. Because the available energy of a SC is proportional to SOC^2, approx. 75% of the SC energy can be used over the charge-discharge range. Here, the min. SOC value at 61% reduces the energy range to ($1–0.61^2$), i.e., 63%.

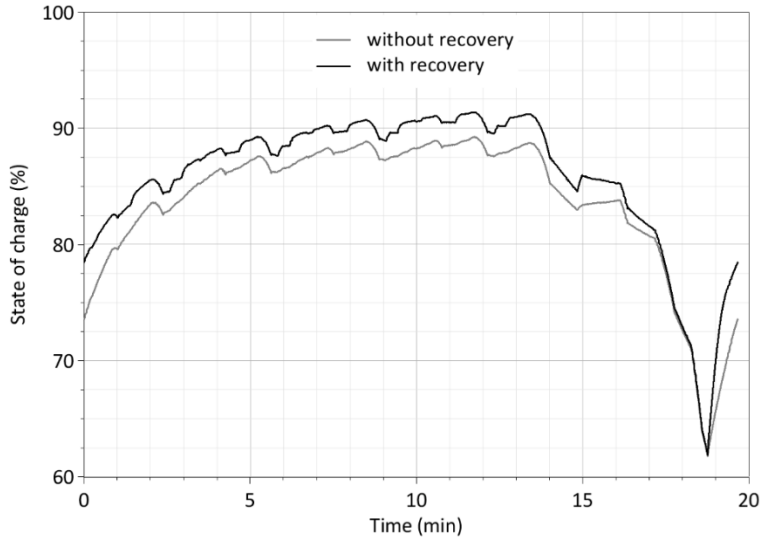

Figure 6. SOC of the storage device along a NEDC driving cycle. Conditions: M = 520 kg, SC capacitance: 165 F, with (in black) or without (in grey) recovery in deceleration.

3.1.3. Transient variations of the cell voltage

Driving cycles result in sudden changes in power demand, thus the fuel cell is to be submitted to sharp current and voltage variations. From the experimental data, we tried to estimate the change in individual cell voltage induced by the cycling procedure, with and without hybridization. For this purpose, the filtered variations of the cell voltage were numerically derived using a centered scheme with upward and downward V value over a 2 second period: the voltage rate obtained was then divided by the number of cells in the system, i.e., 160 cells. Comparison was made on the hybridization mode, i.e., with or without SC storage device.

The case of a 415 kg vehicle was treated with assistance of the smaller (110 F) SC. As shown by Figure 7a, for the 415 kg vehicle motioned by the hybrid source without regeneration, the max. voltage scan rate is in the order of 5 mV/s (positive) and −4 mV/s (negative). The positive voltage rate corresponds to a current rate of −2.5 A/s, i.e., 3.8% of the nominal current range, which indicates an acceptable stress of the fuel cell after [5,12].

For the sake of comparison, the behavior of the fuel cell alone was simulated, starting from the raw data of the power of the above hybrid source. The maximum power of the hybrid source was at 12 kW, with a maximum FC power near 5.5 kW. Therefore, we considered here the only fuel cell power estimated as homothetic from the HS source power, with a factor (5.5/12), assuming the hybridization effect be independent of the overall power. According to this scenario, the fuel cell was modelled for traction after the NEDC driving cycle, but M had then to be reduced to 183 kg vehicle assuming the maximum consumption near 30 W/kg (Table 1) calculated regardless of hybridization mode. The fuel cell was modeled using the steady state relationship between current and voltage established above. For each time value, fuel cell power P, taken as its measured value, was expressed as a function of V and I:

$$P_{FC} = V \times I = V(I) \times I \quad (6)$$

where V was expressed versus I after rel. (6). Current I was estimated by a trial and error technique to find the zero of function F(I) defined as:

$$F(I) = P_{FC} - V(I) \times I \quad (7)$$

From the time variations of the stack voltage, numerical derivation of the voltage signal was performed, leading to Figure 7b: the graph in the figure exhibits more than ten positive peaks of cell voltage scan rate, with amplitude larger than 50 mV/s/cell, plus one attaining 140 mV/s/cell. The corresponding current rates were near −16 and −47 A/s, i.e., 25 and 73% of the nominal FC current range, expressing the significant stress of NEDC cycles exerted on the non-hybridized fuel cell. The rates of negative FC voltage variation are of a lower amplitude, being in all cases below −40 mV/s. Nevertheless, the two graphs above demonstrate that hybridization has a significant smoothing effect on the cell voltage in change in the power demand profiles, which is to reduce the significance of the stress on the fuel cell stack in NEDC cycling operation. This represents a significant asset of hybridization, in addition to the different weights of the vehicle considered for an equivalent fuel cell rated power, i.e., 183 kg without hybridization and 415 kg with the lighter hybridization mode.

3.2. Effects of the hybridization mode and vehicle weight

In this section, recovery of the deceleration power was not accounted for in the experiments. Six series of cycles have been recorded, for weight M ranging from 400 to 520 kg, and depending on the SC storage device capacitance (110 F and 165 F). The average and maximum power of the hybrid source are linear functions of the weight of the vehicle, as demonstrated above, regardless of the hybridization mode, provided that the source is powerful enough to move the vehicle in the whole driving cycle. Therefore, the average power delivered by the fuel cell is also independent of the SC capacitance (see Figure 8a, mean FC powers obtained at 110 F and 165 F, for M = 400 kg).

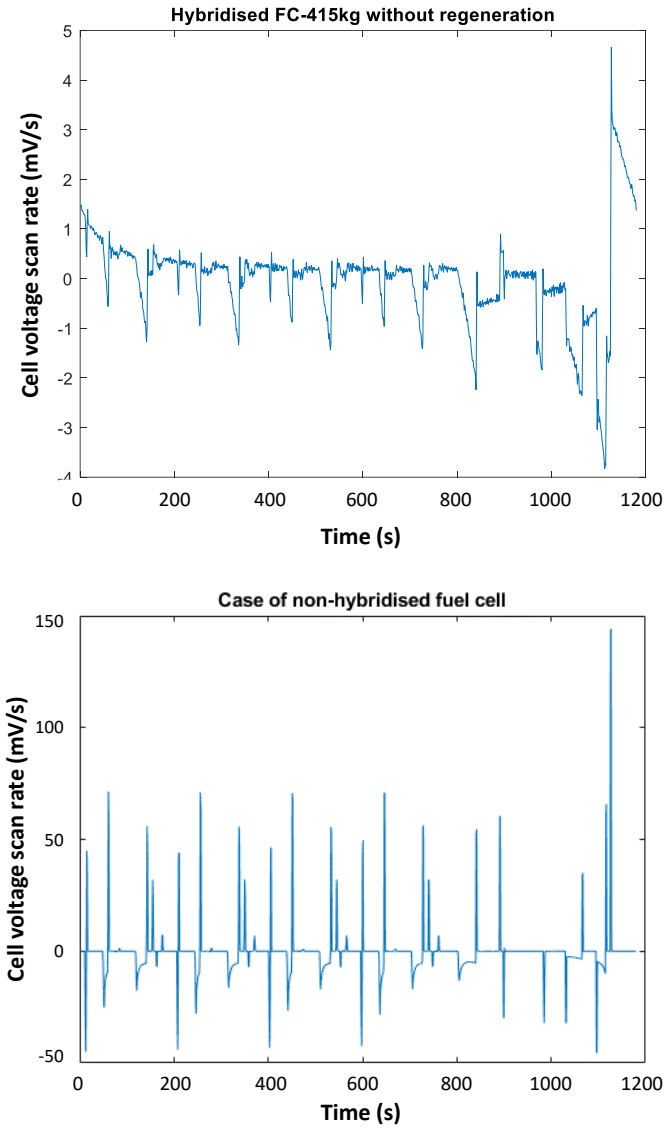

Figure 7. Numerical derivatives of the single cell voltage of the FC system in the NEDC driving cycle. (a): M = 415 kg, no recovery in deceleration, hybridization with 110 F SC storage device. (b): fuel cell alone, with the same max. power (5.50 kW, obtained with M = 183 kg).

On the contrary, the peak power delivered by the FC depends on both the vehicle weight and the SC capacitance: as expected, large capacitances facilitate the driving cycle, then a lower maximum power of the fuel cell is thus required. For instance, as seen in Figure 8a, the maximum power requirement of the FC at 400 kg–165 F is 18% lower than that with 400 kg–110 F. This gain in power capabilities is also apparent in Figure 8a at FC rated power (obtained for 415 kg–110 F and 520 kg–165 F), with a 25% increase in HS maximum power. From the plotted data, the global hybridization ratio defined as $P_{HS,MAX}/P_{FC,MAX}$, was found equal to 2.15 with the 110 F SC device, and in the narrow range 2.67–2.78 with the larger 165 F SC module with approx. 20% increase in the vehicle weight.

Considering heavier vehicles forces the fuel cell to work with a higher intensity, as observed for instance with the 165 F SC device (Figure 8b). In addition, the larger the SC capacitance, the more

pronounced is to be the smoothing effect of hybridization, resulting in particular in larger minimum currents and lower maximum currents. The two cases with 415 kg and 520 kg with different SC capacitances were designed to approach the largest vehicle weight for the two considered hybridizations, resulting in max. FC currents close to 63 A (Figure 8b).

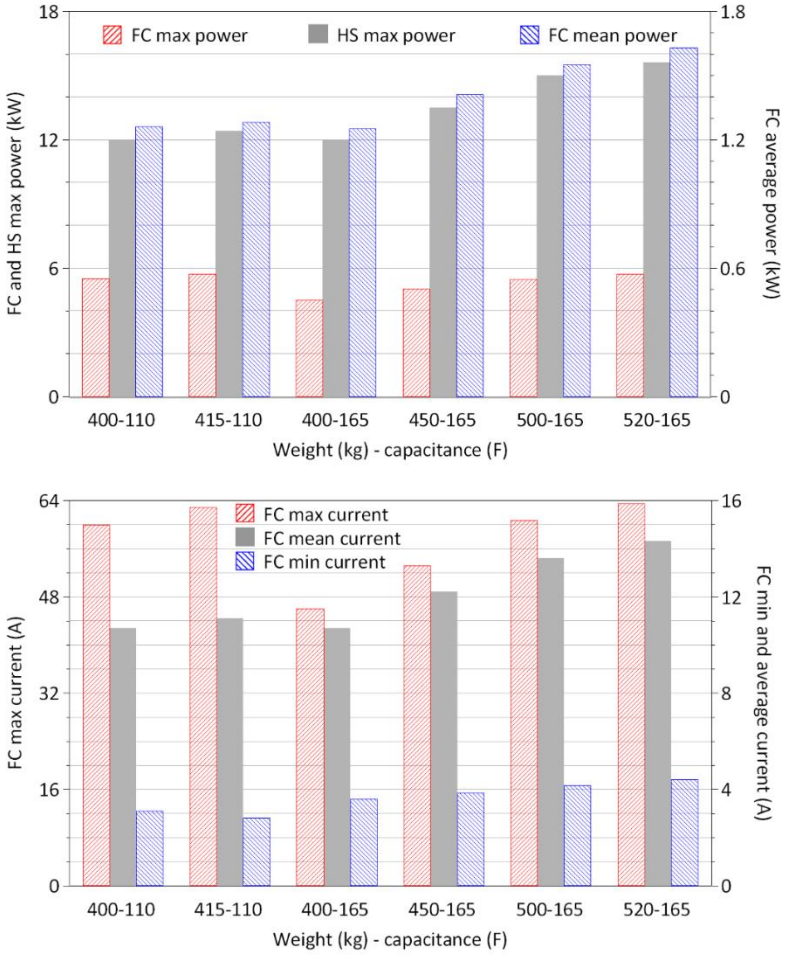

Figure 8. Hybrid source features vs vehicle weight and the SC capacitance. Top (a): average FC power, maximum FC and HS powers. Bottom (b): minimum, average and maximum FC currents. Conditions: no recovery in deceleration.

In accordance with the currents generated by the fuel cell, the voltage values per single cell are reported in Figure 9a. The maximum single cell voltage varied in the range 0.81 V–0.83 V. Finally, the extreme values of the SC state of charge were moderately affected by the vehicle weight and the capacitance of the SC module, varying from 0.61 to 0.66 (Figure 9b). As expected, the larger SC capacitance makes the direct hybridization easier for the HS components, thus its corresponding SOC varied within a narrower range than with the smaller capacitance. Moreover, increasing weight M imposes more stress to the hybrid source components, as expressed by lower values for the min. SOC values (Figure 9b), being not far from the min. affordable value near 61%.

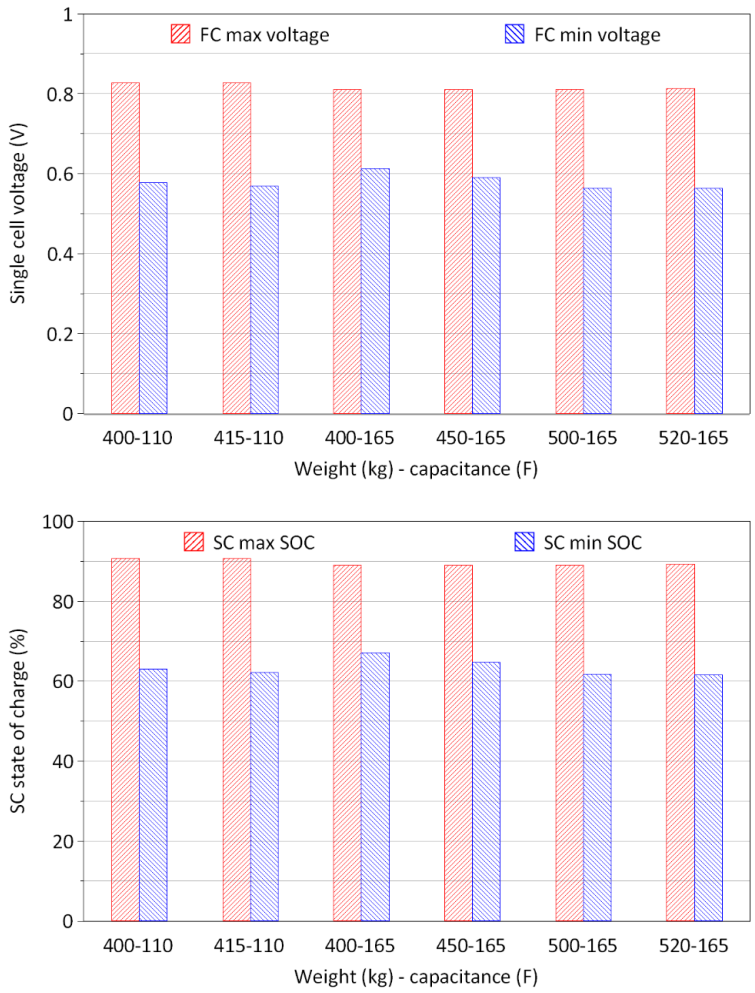

Figure 9. Hybrid source features vs vehicle weight and the SC capacitance. Top (a): minimum and maximum FC voltage. Bottom (b): minimum and maximum SC states of charge. Conditions: no recovery in deceleration.

3.3. Effect of the recovery of the deceleration power

Recovery of deceleration power changes drastically the time profiles of the hybrid source power (see red profile in Figure 3, and grey profile in Figure 5b). The four cases with the 165 F SC stack have been examined here, with or without recovery during deceleration, for comparison. In agreement with the model statement, the experimental maximum power of the hybrid source was not changed by the strategy for power recovery. On the contrary, the power demand from the fuel cell could be reduced by the recovery of the deceleration power. This is clearly shown in Figure 10a by the 24% reduction in the average FC power.

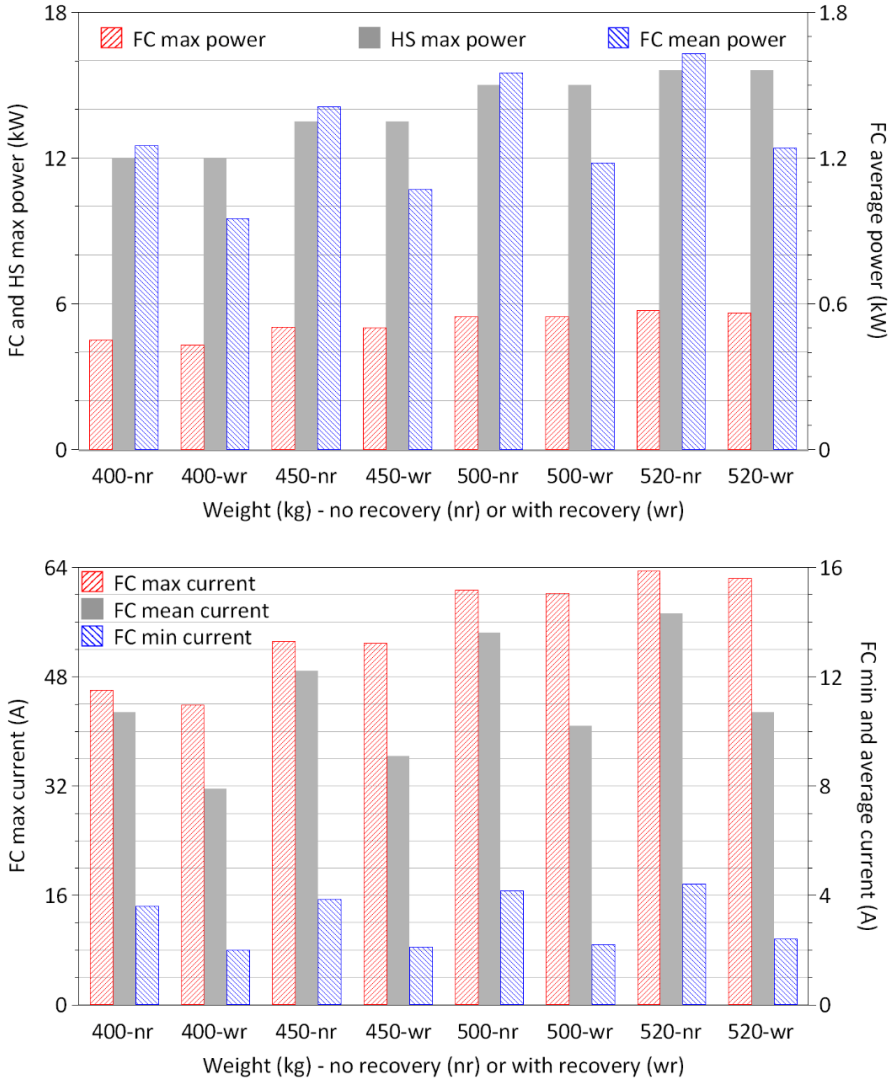

Figure 10. Hybrid source features vs vehicle weight and strategy for power recovery. Top (a): average FC power, maximum FC and HS powers. Bottom (b): minimum, average and maximum FC currents. Conditions: SC capacitance = 165 F.

The effect of recovery appears also clearly in Figure 10b on the minimum and average currents of the fuel cell: as predicted by the model, this last current was reduced by 25%, with an equivalent reduction in hydrogen consumption as a direct consequence. The effect on FC maximum power is however much less significant, being only 2% lower, due to a slight increase in the storage device minimum SOC, from 61% to 63% (cf. Figure 11b) which indicates that recovery of this power has no significant impact on HS power capabilities.

The slight reduction in FC minimum current (about 2 A reduction) can be related to the maximum fuel cell voltage, which was slightly larger, approx. 20 mV per cell, than without recovery (Figure 11a).

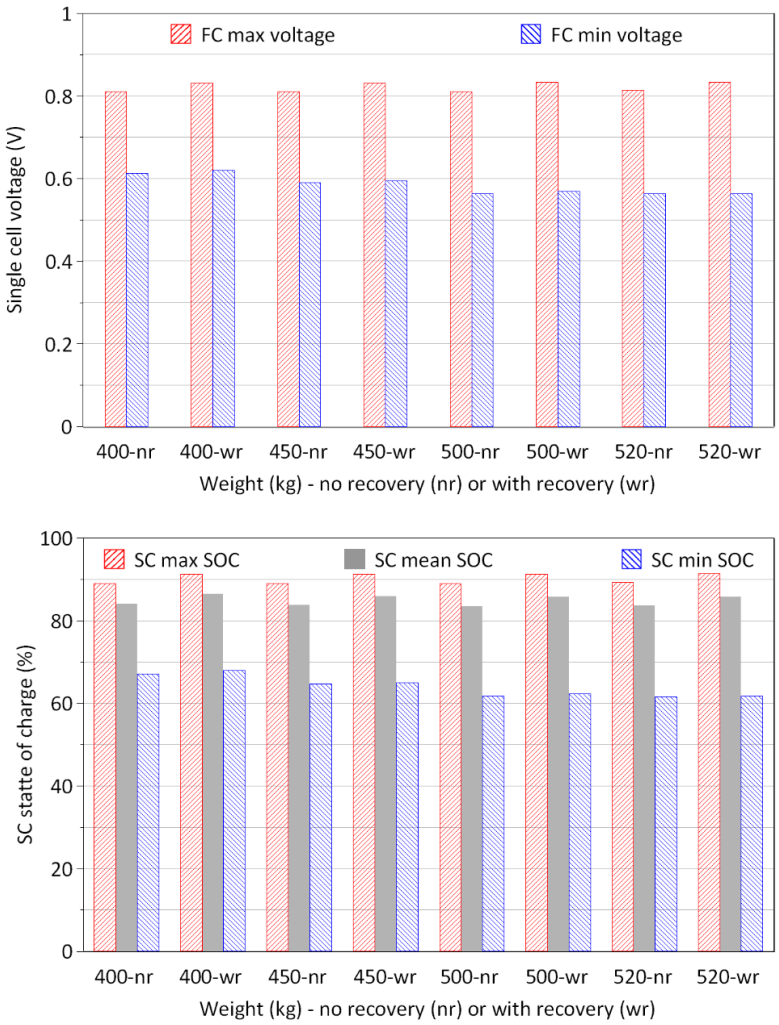

Figure 11. Hybrid source features vs vehicle weight and strategy for power recovery. Top (a): minimum and maximum FC voltage. Bottom (b): minimum, average and maximum SC states of charge. Conditions: SC capacitance = 165 F.

Although allowing an appreciable gain in energy efficiency, the recovery may slightly impact the durability of the fuel cell because of the slightly larger potential of the cathode accompanied by more pronounced corrosion phenomena of the catalyst layer [3,4]. However, the maximum voltage observed near 0.83 V, is below the OCV attained by the non-hybridized fuel cell in the idle periods of the cycle. With concern to the minimum cell voltage, the effect of the power recovery strategy is more restricted, the main effect from the operating conditions being that from the vehicle weight. Finally, SOC levels of the SC storage device directly linked to the fuel cell voltage, were slightly affected by this recovery (Figure 11b) with approx. 2% absolute increase in max. and average SOC values, and no visible effect on the minimum SOC.

4. Conclusions

On the basis of experimental results obtained with laboratory fuel cells, and a model for the direct hybrid (FC-SC) source, a fuel cell system (145 V, 65 A, 5.6 kW) was directly connected to a

supercapacitor element system with a capacity up to 165 F, for tests emulating the ride of a fictitious vehicle in NEDC cycles for suburban transport.

As observed at small scale, the profile of the FC current is greatly smoothed by direct hybridization to supercapacitors. In addition, the estimated voltage scan rate estimated by derivation of the measured voltage transient, exhibited several peaks above 50 mV/s per single cell without hybridization, but was shown to be lower than a few mV/s with the larger SC system. This is to improve the durability of the fuel cell. Because of the restricted range of the fuel cell current density (below 0.4 A/cm^2), SOC of the SC varied in a moderate range, however without compromising the principle of the hybridization. The vehicle weight was restricted as expected by the power and energy of the hybrid source, depending on the capacity of the SC storage system. With or without recovery of the deceleration power, NEDC cycles can be completed with a 520 kg "Zoe-like vehicle" powered by the 15.6 kW hybrid source with 165 F with a SC weight at 81 kg. This validated the formerly calculated rating power of direct (FC-SC) source near 30 kW for a one-ton vehicle [23]. The main effect of deceleration power recovery is fuel saving, up to 25% in NEDC cycle conditions.

Scaling-up of the results presented to real driving conditions can be done with an individual H_2-car upon installation of the supercapacitor system. A 10–12 kW rated fuel cell could suffice in the traction of a one-ton vehicle in suburban rides. Ideally, its nominal voltage would exceed 100 V, in order to reduce as much as possible, the voltage conversion between the source and the electric engines, for nominal currents below 150 A, allowing reasonable currents from the hybrid source. Such conditions are however seldom fulfilled by FC currently on the market, usually with nominal 50 V–300 A. The emerging transport route developed here could be the incentive to design and construct fuel cells more suitable to this large potential application, also permitting diversification of the membrane fuel cell market.

Besides, water-cooled fuel cells—as used in H_2-cars—offer broader ranges of current density and power that the cell used in this study, making it possible to widen the SOC range of the storage elements in the cycle. Thus, the capacity of the SC system could be substantially reduced, or kept unchanged should the ratio SC capacity/FC power be kept, which would result in a higher flexibility in the transport: changes in the standardized power profiles such as longer peaks, or existence of slopes in the ride could then be envisaged. Nevertheless, in the design of the hybrid source, a compromise has to be found between flexibility in the ride, and the weight and volume requirement of the SC storage system. In any case, the transport solution developed here with storage elements free from lithium and rare earth elements, has to be mainly considered for routine suburban transport in relatively flat areas, for private or shared use, as a dedicated alternative to other currently developed transportation solutions being more energy- and critical metal-demanding.

Acknowledgements

This work was supported by the French PIA project «Lorraine Université d'Excellence», reference ANR-15-IDEX-04-LUE, ATMO agency for Air Quality, France, and European Union (FEDER).

Conflict of interest

The authors declare no conflict of interest.

Author contributions

CB: Project management, supervision, SR: Conceptualization, setup design and implementation, Writing—review and Editing, MH: Methodology, SG: Setup design and implementation, TH: Fuel cell control, JV: Fuel cell control, XF: Setup installation, MCP: Formal analysis, FL: Writing—review and Editing.

References

1. Fathabadi H (2018) Fuel cell hybrid electric vehicle (FCHEV): novel fuel cell/SC hybrid power generation system. *Energy Convers Manage* 156: 192–201.
2. Sampietro JL, Puig V, Costa-Castelo R (2019) Optimal sizing of storage elements for a vehicle based on fuel cells, supercapacitors, and batteries. *Energies* 12: 925.
3. Lapicque F, Bonnet C, Huang BT, et al. (2012) Analysis and evaluation of aging phenomena in PEMFCs. In: K. Sundmacher, *Advances in Chemical Engineering*. 41: 265–330.
4. Zhang S, Yuan XZ, Hin JN, et al. (2019) A review of accelerated stress tests of MEA durability in PEM fuel cells. *Int J Hydrogen Energy* 34: 388–404.
5. Carignano MG, Costa-Castello R, Roda V, et al. (2017) Energy Management strategy for fuel cell-capacitor hybrid vehicles based on prediction of energy demand. *J Power Sources* 360: 419–433.
6. Wu B, Parkes MA, Yufit W, et al. (2014) Design and testing of a 9.5 kW proton exchange membrane fuel cell-supercapacitor passive hybrid system. *Int J Hydrogen Energy* 39: 2885–2896.
7. Yeersorn R, Maiket Y, Kaewmanee W (2020) The observation of supercapacitor effects on PEMFC-supercapacitor hybridization performance through voltage degradation and electrochemical processes. *RSC Advances* 10: 13100–13111.
8. Ahmadi S, Bathaee SMT, Hosseinpour AH (2018) Improving fuel economy and performance of a fuel-cell hybrid electric vehicle (fuel-cell, battery, and ultra-capacitor) using optimized energy management strategy. *Energy Convers Manage* 160: 74–84.
9. Macias A, Kandidayeni M, Boulon L, et al. (2020) Passive and active coupling comparison of fuel cell and supercapacitor for a three-wheel electric vehicle. *Fuel Cell* 20:351–361.
10. Jacome A, Depature C, Boulon L, et al. (2021) A benchamrk of different starting modes of a passive fuel cell/ultracapacitor hybrid source for an electric vehicle application. *J Energy Storage* 35: 102280.
11. Depature C, Macias A, Jacome A, et al. (2020) Fuel cell/supercapacitor passive configuration sizing approach for vehicular applications. *Int J Hydrogen Energy* 45: 26501–26512.
12. Xun Q, Lundberg S, Liu Y (2021) Design and experimental verification of a fuel cell/supercapacitor passive configuration for a light vehicle. *J Energy Storage* 33: 102110.
13. Tsotridis G, Pilenga A, de Marco G, et al. (2015) EU harmonised test protocols for PEMFC MEA testing in single cell configuration for automotive applications. *In JRC Science for Policy report EUR* 27632 EN.
14. Andre M, Keller M, Sjödin A, et al. (2008) The Artemis European tools for estimating the pollutant emissions from road transport and their application in Sweden and in France. *Proceedings of the 17th Conference "Transport and Air Pollution"*, Graz 2008.
15. United State Environmental Protection Agency, EPA dynamometric drive schedules. URL: https://www.epa.gov/vehicle-and-fuel-emissions-testing/dynamometer-drive-schedules.

16. Hinaje M, Raël S, Caron JP, et al. (2012) An innovating application of PEM fuel cell: current source controlled by hydrogen supply. *Int J Hydrogen Energy* 37: 12481–12488.
17. Silva RE, Harel F, Jemei S, et al. (2014) Proton exchange membrane fuel cell operation and degradation in short-circuit. *Fuel Cell* 14: 894–905.
18. Chandesris M, Vincent R, Guetaz L, et al. (2017) Membrane degradation in PEM fuel cells from experimental results to semi empirical degradation laws. *Int J Hydrogen Energy* 42: 139–149.
19. Pei P, Chang Q, Tang T (2008) A quick evaluating method for automotive fuel cell lifetime. *Int J Hydrogen Energy* 33: 3829–3836.
20. Gérardin K, Raël S, Bonnet C, et al. (2018) Direct coupling of PEM fuel cells to supercapacitors for higher durability and better energy management. *Fuel Cell* 18: 315–325.
21. Arora D, Bonnet C, Mukherjee M, et al. (2019) Direct hybridization of PEMFC and supercapacitors: Effect of excess hydrogen on a single cell fuel cell durability and its feasibility on fuel cell stack. *Electrochim Acta* 310: 213–220.
22. Arora D, Bonnet C, Mukherjee M, et al. (2020) Long term study of directly hybridized proton exchange membrane fuel cell and supercapacitors for transport applications with lower hydrogen losses. *J Energy Storage* 23: 101205.
23. Arora D, Hinaje M, Raël S, et al. (2018) Sizing supercapacitor for direct hybridization with polymer electrolyte membrane fuel cell. *Proceedings of the IEEE-VPPC Conference*, Chicago 2018.
24. Arora D (2019) Direct hybridization of a PEM fuel cell and a supercapacitor storage device: Comparative study of aging in urban cycling, and optimal management of hydrogen consumption PhD dissertation, University of Lorraine, France.
25. Noiying P, Hinaje M, Thouthong P, et al. (2012) Using electrical analogy to describe mass and charge transport in PEM fuel cell. *Renewable Energy* 44: 128–140.
26. Belhachemi F, Raël S, Davat B (2000) A physical based model power electrical double layer capacitors. *Proceedings of the Conference Record of the 2000 IEEE Industrial Applications Systems*, 3039–3076.
27. Buller S, Karden E, Kok D, et al. (2002) Modeling the dynamic behavior of supercapacitors using impedance spectroscopy. *IEEE Trans Ind Appl* 38: 1622–1626.

AIMS Press